DETAILED STUDY OF ELECTROMIGRATION INDUCED DAMAGE IN Al AND AlCuSi INTERCONNECTS

U.E. Möckl, M. Bauer, O. Kraft, J.E. Sanchez Jr.*, and E. Arzt
Max-Planck-Institut für Metallforschung and Institut für Metallkunde, University of Stuttgart, Stuttgart, Germany; *Advanced Micro Devices, Sunnyvale, CA

ABSTRACT

Because of the continuing miniaturization, electromigration (EM) phenomena are still a key issue in reliability of VLSI metallizations. The present study of EM induced voiding and hillocking was performed on unpassivated conductor lines with various widths and current densities. Stressed and unstressed interconnects were carefully examined with SEM and TEM techniques, especially with regard to void densities, void sizes and characteristic lengths between void and hillock. The fatal void shape was related to current density and line width indicating that the failure mechanism changes with decreasing line width and decreasing current density.

INTRODUCTION

The phenomenon of electromigration (EM) seemed to be understood if not quantitatively so at least qualitatively. But, recent experimental results[1,2] in passivated lines showed a transition from the common wedge-shaped voids to slit-like, in some cases even transgranular voids with decreasing line widths and current densities. The question arose if equivalent changes in void morphology could be found in unpassivated samples as well. Thus in this paper a quantitative analysis of void morphology, void density and the spacing between corresponding voids and hillocks is presented. Moreover, we discuss the difference between two sample lots (Al and AlCuSi) made from different laboratories.

EXPERIMENTAL

Sample preparation was performed in two different laboratories to examine the influence of 'quality' on basic electromigration behavior. The Al films (0.5 μm thick) were sputter deposited onto thermally oxidized silicon wafers[3]. Films were annealed in forming gas at 400°C for 45 minutes. The Al-0.5%Cu-1%Si films were sputter deposited, too, with a thickness of 0.85 μm. Parallel line arrays (PLA) of 20 lines 1 mm long were patterned using standard lithographic and etch processes. The AlCuSi samples[4] were annealed before testing in forming gas at 480°C for ca. 20 min. to provide the same starting conditions for all tests (precipitation structure, grain size). Both types of samples were unpassivated.

EM testing was performed on wafer level using a current source operating under constant voltage conditions. This method is necessary to not destroy the failure sites by arcing as the line produces an open circuit. Test temperature for all tests was 227°C. Different conditions were used (either constant line width with varying current densities or constant current density with varying line width ⇒ Table 1).

Table 1: Samples and test conditions

	Al	AlCuSi
Current density (j)	1–1.9 MA/cm^2 *(w=1.4 μm)*	0.71–2.72 MA/cm^2 *(w=1.9 μm)*
Line width (w)	1–4.8 μm *(j=2.4 MA/cm^2)*	1.05–3.8 μm *(j=2.16 MA/cm^2)*

At the highest current densities considerable Joule heating (ca. 15°) was produced. Therefore, the measured median time to failures (MTF) were modified to get the same standard (with the help of Black's equation[5] using an activation energy of Q=0.6 eV). Grain size was measured as 1.8 µm for Al and 1.91 µm for AlCuSi in the continuous film. After EM testing samples were observed in a scanning electron microscope (SEM). The whole length of each line was examined carefully for damage sites and a micrograph was taken of each fatal void. The distance to the next (downstream) hillock was measured too. Additional methods used to characterize either continuous films or conductor lines were nanoindentation, wafer curvature and transmission electron microscopy (TEM).

RESULTS

Tests with Varying Current Densities

Both MTF and median void-hillock distances (VHD) show a strong dependence on current density. In Figures 1 and 2 these quantities are plotted for Al and AlCuSi respectively. The fitting curves follow a j^{-n} relationship (for MTF and VHD). The values for n are summarized in Table 2. N-values for MTFs lie between 3 and 4 (somewhat higher than the often reported value 2)[6]. The distances between voids and hillocks are approximately inversely proportional to current density.

Table 2: n-values

n	MTF	Void-Hillock
Al	3.92	1.47
AlCuSi	3.28	0.87

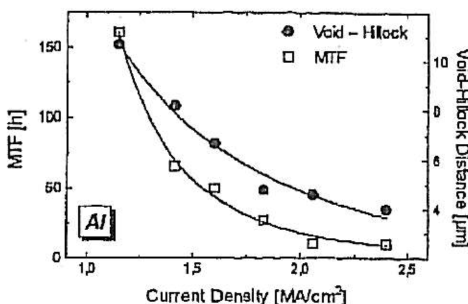

Figure 1: MTF and void-hillock distance vs. current density for Al

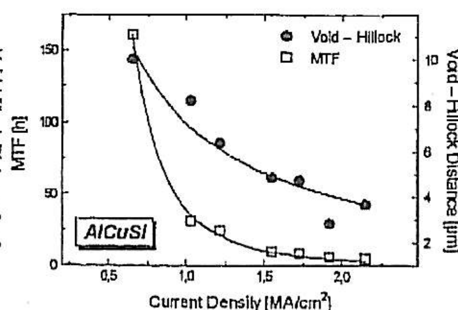

Figure 2: MTF and void-hillock distance vs. current density for AlCuSi

To quantify the extent of damage for different films and current densities, the 'void density', defined as the total number of voids divided by the entire area of lines in the PLA circuit, is shown in Figure 3. The void density decreases with decreasing current density for both alloys and is 5-10 times higher for the AlCuSi samples.

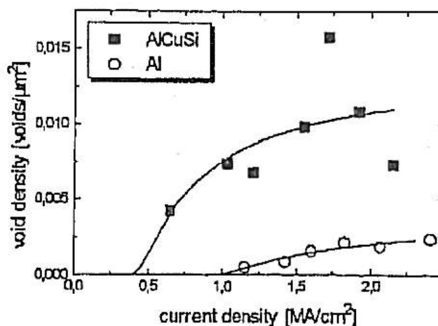

Figure 3: Void density vs. current density

Tests with Varying Line Widths

Figures 4 and 5 show the MTF and the void-hillock distance versus the ratio line width to grain size (w/g). Both sample lots show the

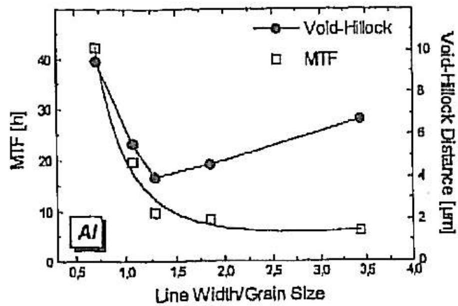

Figure 4: MTF and VHD vs. w/g for Al

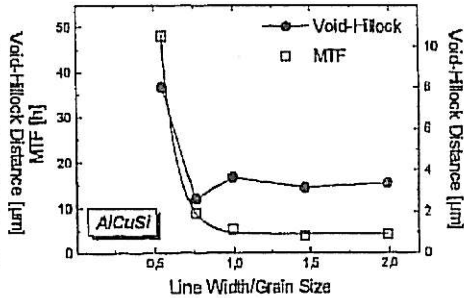

Figure 5: MTF and VHD vs. w/g for AlCuSi

often seen sharp increase in MTF as w/g falls below 1. The VHDs show an increase for smaller w/g which corresponds to the increase in MTF. For w/g bigger than 1 the VHDs grow slightly (for Al more than for AlCuSi).

Void Shape as a Function of Stressing Conditions

The SEM observations revealed a change in fatal void shape under different stressing conditions. Two different groups of fatal void shapes could be distinguished: wedge-like and slit-like voids. Typical examples for both types are illustrated in Figure 6.

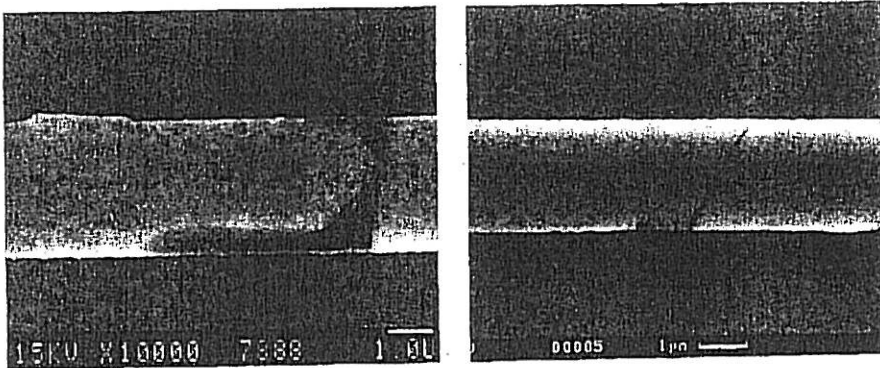

Figure 6: left side: wedge shaped fatal void; right side: slit-like fatal void

Figures 7 and 8 illustrate the effect of current density and line width on the percentage of slit failures. The amount of slit failures changed with stressing conditions, it increased steadily with decreasing current density and more rapidly with decreasing w/g. It is evident that slit failures are more common for AlCuSi than for Al samples.

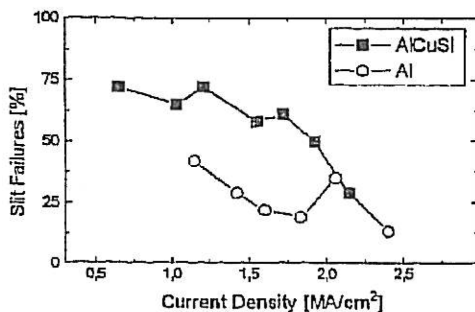

Figure 7: Percentage of slit failures vs. j

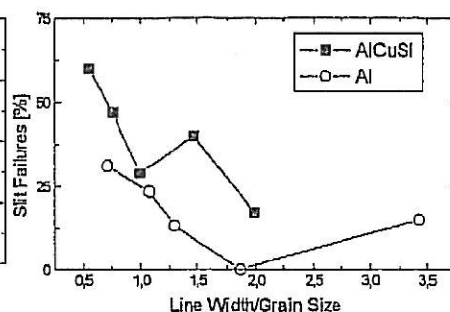

Figure 8: Percentage of slit failures vs. w/g

DISCUSSION

Current Density as a Variable

Due to a back driving force caused by a stress gradient ('Blech effect'), a 'critical' threshold product can be defined which must be exceeded for damage to form (voids or hillocks)[7]:

$$(j \cdot l)_c = \frac{\sigma^* \Omega}{eZ^* \rho} \tag{1}$$

Here is σ^* the maximum hydrostatic stress the metallization is able to sustain, Ω the atomic volume, eZ^* the effective charge of the atom, ρ the electrical resistivity and l the length of the 'Blech stripe'.

Converted to conductor stripes, this formalism means that there should be no evidence of EM damage formation in lines shorter than the critical length l_c and, more important, that in the case of near-bamboo grain structures only those sites are able to nucleate a void that have a continuous grain boundary path (polygranular segment) longer than the critical length. Then, failure will occur in one of those long polygranular segments.

The reason for the experimental result (Fig. 1 and 2) that the median distance fatal void to next hillock (the distribution is lognormal[3]) approximately inversely proportional to j is, is now clear: the current density fixes l_c and limits the range of possible segments. Accompanied by the increase of the VHD with decreasing j is an increase of the MTF.

The question arises if it is possible to make an estimate of the critical current density j_c. Two different evaluations are possible: recent experimental and theoretical work[4,8,9] suggests the following relation between MTF and j:

$$MTF \propto \frac{1}{(j - j_c)^2} \tag{2}$$

A fit with this function showed excellent agreement with our data. The second method uses a result from computer modeling of grain growth in conductor lines[10]. Walton et. al. found that the distribution of polygranular segment lengths can be written as

$$C(l) = l_a^{-2} \exp(-l/l_a) \tag{3}$$

where C is the number of segments with length l and l_a is the average segment length. From this equation the total number of segments N longer than a critical length l_c can be computed[2]:

$$N(l > l_c) = N_0 \exp(-l_c/l_a) \tag{4}$$

where N_0 is the total number of segments in the line. N can be correlated with the void density when it is assumed that every segment longer than l_c forms a void. Then the void density should show the following dependence:

$$VD \propto \exp\left(-\frac{A}{j-j_c}\right) \quad (5)$$

where VD is the void density and A is a constant. The fit is included in Fig. 3. The results from both analyses are summarized in Table 3. The values agree surprisingly well. The j_c value for Al is about 2 times higher than the corresponding value for AlCuSi. This is consistent with the observations that the lifetime of the AlCuSi samples is smaller than the lifetimes for pure Al samples, that the VHDs are smaller for AlCuSi and that the void density is 5 to 10 times higher for AlCuSi.

Table 3: Critical current densities

j_c [MA/cm^2]	Al	AlCuSi
MTF method	0.67	0.34
Void Density method	0.79	0.32

These results were very surprising, because they would indicate a harmful influence of alloying elements on EM resistance, which was never seen elsewhere (besides some observations in narrow passivated lines[11]). Of the parameters which could affect the threshold product and the void density σ^* can in principle be influenced by a number of effects. In our case this could be a strengthening effect of the Al film due to its smaller thickness. But nanoindenter and wafer curvature measurements showed only a slightly higher mechanical strength in the continuous films. The perhaps by far most important effect can be ascribed to the 'quality' of the samples. Precipitates can usually serve as sites for heterogeneous nucleations of voids[12,13]. The same effect could be provided by impurities introduced by a less clean sputtering environment. If these impurities lower the nucleation barrier for voids the higher void densities in AlCuSi can be explained. Another consequence is that the threshold product for EM damage formation is reduced. This tentative explanation would also be consistent with recent X-ray stress measurements that showed unexpected high stress relaxation in lines that had been deliberately 'strengthened' by oxide particles through ion implantation[14].

Line Width as a Variable

The increase of MTF below w/g≈1 is often seen and indicates usually the transition from a continuous grain boundary network to a bamboo structure. The VHD increase below w/g=1 is a consequence of the accompanying decrease of the average cluster length[2]. In Equation (4) it can be seen that a decrease of the average cluster length is followed by a reduction in the total number of segments longer than l_c. Hence, the number of possibilities to form a void is reduced and the MTF should rise. This effect is no longer valid if there are no longer polygranular segments of sufficient length. In this case new diffusion paths need to be considered, e.g. volume or dislocation core diffusion, and the sites where flux divergencies could arise are unknown.

The behavior of VHD for w/g bigger than 1 is nonuniform: Al shows an increase and AlCuSi stays constant. In wider lines with a continuous grain boundary network material can be transported over longer distances. Possible flux divergency sites are now no more blocking grains but e.g. grain boundary triple points. Hence, VHDs should increase with widening of the conductor lines because of an increasing number of paths along the line. However, in the case of alloys the precipitates can serve as barriers. Therefore the VHD would be expected to be approximately independent of line width for wide lines with alloying elements.

Void Shape – Damage Map

Slit failures are, especially for the AlCuSi samples, the dominant failure morphology for narrow lines and small current densities. The alloying seems to intensify this trend but the reasons are not fully understood.

The fact that tests were performed with varying current densities and varying line widths provide the possibility to construct an experimental damage map (Figure 9). In this map the lower left corner is the field of the slit failures. Theoretical modeling makes it possible to explain some of these observations[15].

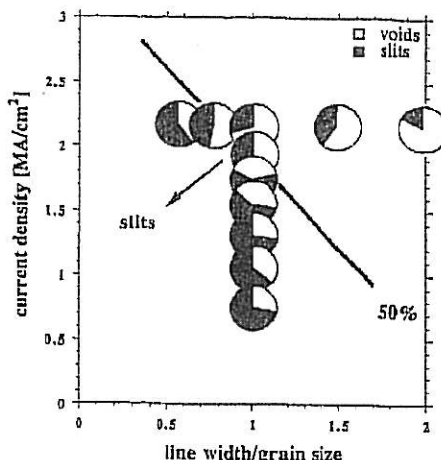

Figure 9: Damage map for slit failures as function of j and w/g for AlCuSi

CONCLUSIONS

- Slit failures dominate the low current density - narrow line width region. It is possible to construct a damage map for slit failures. The void morphology of unpassivated samples thus resembles that of passivated lines.
- The variation of void-hillock distances with current density and line width correlate with the MTF and can be explained with the help of Blech's equations. The threshold current densities were extracted from the data with two different methods and showed excellent agreement (for Al $j_c \approx 0.67\text{-}0.8$ MA/cm^2 and for AlCuSi $j_c \approx 0.33$ MA/cm^2).
- A comparison between Al and AlCuSi (made at different production facilities) revealed a poorer EM resistance for AlCuSi, which must be interpreted as difference in quality. However, the basic EM behavior of both sample lots is comparable.

REFERENCES

1. J.H. Rose, and T. Spooner, *Mater. Res. Soc. Symp. Proc.* **309**, 409 (1993).
2. E.M. Atakov, J.J. Clement, and B. Miner, *Mater. Res. Soc. Symp. Proc.* **309**, 133 (1993).
3. O. Kraft, J.E. Sanchez Jr., and E. Arzt, *Mater. Res. Soc. Symp. Proc.* **265**, 119 (1992).
4. M. Bauer, *Diploma Thesis*, University of Stuttgart, 1993
5. J.R. Black, *IEEE Trans. El. Dev.* **16**, 338 (1969).
6. M. Shatzkes, and J.R. Lloyd, *J. Appl. Phys.* **59**, 3890 (1986).
7. I.A. Blech, *J. Appl. Phys.* **47**, 1203 (1976).
8. R.G. Filippi, G.A. Biery, and M.H. Wood, *Mater. Res. Soc. Symp. Proc.* **309**, 141 (1993).
9. E. Arzt, and W.D. Nix, *J. Mater. Res.* **6**, 731 (1991).
10. D.T. Walton, H.J. Frost, and C.V. Thompson, *Mater. Res. Soc. Symp. Proc.* **225**, 219 (1991).
11. E.M. Atakov, A. Shepela, and B. Miner, *Mater. Res. Soc. Symp. Proc.* **309**, 401 (1993).
12. J.E. Sanchez Jr., and E. Arzt, *Mater. Res. Soc. Symp. Proc.* **265**, 131 (1992).
13. A.L. Greer, and W.C. Shih, *Mater. Res. Soc. Symp. Proc.* **265**, 83 (1992).
14. W.-M. Kuschke, and E. Arzt, submitted to *Appl. Phys. Lett.*
15. E. Arzt, O. Kraft, and U.E. Möckl, same volume.